Implicit Shock-Fitting Scheme for Unsteady Transonic Flow Computations

N. J. Yu,* A. R. Seebass,† and W. F. Ballhaus‡
University of Arizona, Tucson, Ariz.

The alternating-direction implicit scheme developed by NASA Ames for unsteady transonic flows has been modified to include a shock-fitting algorithm, as well as an analytically stretched coordinate system. The shock-fitting procedure treats shock waves as discontinuities normal to the freestream. Improvements in shock position and the unsteady pressure distributions are obtained by this modification. The various types of shock motion observed experimentally by Tijdeman are well simulated in calculations using the modified computational scheme. The method for detecting shock-wave formation and the procedure for fitting a moving shock wave are illustrated. Results for an NACA 64A006 airfoil with oscillating quarter-chord flap are presented and discussed.

Introduction

THERE is a need for the numerical simulation of unsteady transonic flows about airfoils in order to predict unsteady aerodynamic loads and to provide an understanding of the behavior of unsteady transonic flowfields. A number of methods[1-11] have been proposed for computing such flows, and there is continuing improvement in the results obtained. This paper describes a shock-fitting procedure,[12] coupled with an implicit finite-difference algorithm,[1,2] which can accurately and efficiently simulate most unsteady transonic flows about thin airfoils.

A major consideration in constructing an algorithm for unsteady transonic flows is the treatment of moving shock waves. Experimental observations of Tijdeman[13,14] indicate that even for simple airfoil motions shock-wave motions can be complicated, and they can affect aerodynamic force and moment variations strongly. Time-linearized methods,[9,10] i.e., methods that assume that the unsteady perturbation is small compared to the basic steady disturbance, presently do not consider shock motions although they can be modified to do so for small shock excursions.[15,16] Time-integration methods[1-8] treat shock waves by "capturing" them, a procedure that can present a number of problems that will be discussed subsequently.

Tijdeman's experiments also indicate that shock motion amplitudes increase with decreasing frequency. This is supported by a simplified analysis of the time-linearized equations.[16] Thus, some of the most interesting transonic flowfields result from low-frequency motion. Explicit finite-difference schemes are not efficient when applied to low-frequency cases because the stability restriction on the time step is substantially more severe than that required for accuracy. As a result, efficient semi-implicit methods[3] and even more efficient fully implicit methods[1,2,7,8] have been developed. Caradonna and Isom[7] use an iterative implicit procedure; i.e., the nonlinear implicit finite-difference equations must be solved at a given time iteratively. In an earlier unpublished study we also used such a procedure. Ballhaus and Steger[1] and Beam and Warming[8] constructed more efficient algorithms that solve the nonlinear equations directly by the solution of simple matrix equations generated by an alternating-direction implicit (ADI) procedure. This method has proven to be so efficient, especially for the calculations with nonuniform mesh distributions, that we now often use it as an alternative to successive line overrelaxation (SLOR) for steady flow calculations.[17,18]

All of these implicit schemes "capture" shock waves; i.e., shock waves evolve automatically as part of the numerical solution. This procedure has several deficiencies associated with it. They can be eliminated, at the expense of coding complexity, by "fitting" shock waves as discontinuities in the flow. Shock capturing produces shock profiles that are distorted in a manner that depends on the truncation errors in the finite-difference scheme. The use of mixed-difference schemes[1,8] can improve the situation for cases in which the flow changes from supersonic to subsonic across the shock. However, when this condition is not satisfied, as in the later stages of pulsating motion of a parabolic-arc airfoil, the differencing cannot be switched across the shock and shock resolution is poor. In any case, shock capturing requires spatial grid spacings, in regions where shock waves are anticipated, which are sufficiently small to resolve the shock waves in a reasonable distance. The grid spacing required to do this is frequently much smaller than that required to resolve flow variable gradients in most of the rest of the flowfield. This also results in an unnecessarily severe time-step restriction because time steps for implicit schemes are chosen such that shocks move less than one spatial grid point per time step.[1,8] This is necessary to preserve both accuracy and stability. Shock fitting removes the large gradients from the finite-difference solution and generally permits equivalent flowfield resolution with fewer grid points, both in space and time. Finally, if shock waves are not treated as discontinuities but are to be captured correctly, the difference equations must be solved in conservation form. This imposes an additional constraint on the construction of finite-difference schemes which can be difficult to satisfy. For example, no fully conservative difference scheme for the full potential equations have been developed yet that can match the convergence reliability and computational efficiency of Jameson's non-conservative "rotated" difference procedure.[19]

In principle, the shock-fitting procedure discussed in this paper could be applied to the full potential equation. For steady flows it may substantially reduce the time required to obtain a converged solution. Here, as a first step, it is applied to a simpler formulation that contains the essential nonlinear unsteady behavior associated with low-frequency transonic flows. Furthermore, the algorithm is simplified by treating

Presented as Paper 77-633 at the AIAA 3rd Computational Fluid Dynamics Conference, Albuquerque, N. Mex., June 27-29, 1977; submitted July 26, 1977; revision received April 17, 1978.

Index categories: Transonic Flow; Nonsteady Aerodynamics; Computational Methods.

*Senior Research Associate. Member AIAA.
†Professor. Associate Fellow AIAA.
‡Research Scientist, NASA Ames Research Center and Aeromechanics Laboratory, U.S. Army AVRADCOM.

the shocks as discontinuities normal to the freestream. The procedures could be generalized to a curved shock with additional programming complexity. Methods of detecting shock formation and of judging the existence of a shock wave in the unsteady flowfield are described.

A production code, LTRAN2, has been developed for the efficient solution of low-frequency transonic flows about airfoils in motion.[2] LTRAN2 is based on the ADI method of Ballhaus and Steger,[1] and is being released on request to industry and government agencies. The modification of the ADI procedure to include shock fitting, which is the main subject of this paper, will improve LTRAN2 significantly. Substantially fewer grid points will be required to achieve equivalent flowfield resolution, and the time-step restriction due to shock motion can be relaxed considerably.

Numerical simulations of various types of shock motions for an NACA 64A006 airfoil with oscillating quarter-chord flap are described. Significant improvements in shock resolution and, consequently, in unsteady pressure distributions are obtained using the shock-fitting procedure. The results show the marked effect of shock-wave motion.

Formulation of Governing Equations

Low-Frequency Approximation

The unsteady, small-disturbance, transonic equation for low frequency commonly is written as

$$-2KM_\infty^2\phi_{xt}+\{1-M_\infty^2-(\gamma+1)M_\infty^2\phi_x\}\phi_{xx}+\phi_{yy}=0 \quad (1)$$

which may be derived[20] from a systematic expansion of the velocity potential with respect to the thickness ratio τ and the reduced frequency K, where $K=\omega c/U$, i.e., the angular frequency multiplied by the time that it takes the flow to traverse the airfoil chord. The spatial coordinates, the time, and the velocity potential in Eq. (1) have been nondimensionalized by the chord c, the inverse of the angular frequency ω^{-1}, and Uc, respectively.

The tangency condition and the unsteady pressure coefficient that are consistent with the low-frequency approximation are

$$\phi_y=\frac{\tau\partial Y(x,t)}{\partial x}=\tau\left[Y_{s_x}+\frac{\delta}{\tau}(Y_{u_x}+Y_{u_t})\right] \quad (2)$$

and

$$C_p=-2\left\{\frac{M_\infty^2-1}{(\gamma+1)M_\infty^2}+\phi_x\right\}$$

where $Y(x,t)$, the instantaneous body shape, has been decomposed into a steady part Y_s and an unsteady part Y_u.§ Here δ is the amplitude of the unsteady oscillation. Note that C_p is defined such that, at sonic conditions, $C_p=C_p^*=0$.

Any shock wave that exists in the flowfield must satisfy the jump relation derived from the conservative form of the governing equation (1), viz.,

$$-2KM_\infty^2[\![\phi_x]\!]^2\left(\frac{dx}{dt}\right)_s-\{1-M_\infty^2-(\gamma+1)M_\infty^2\tilde{\phi}_x\}[\![\phi_x]\!]^2+[\![\phi_y]\!]^2=0 \quad (3)$$

together with the condition derived from the assumption of irrotationality,

$$\left(\frac{dy}{dx}\right)_s=-\frac{[\![\phi_x]\!]}{[\![\phi_y]\!]} \quad (4)$$

Here $\tilde{\phi}_x$ refers to the mean value of ϕ_x evaluated on each side of the discontinuity, $[\![\phi_x]\!]$ indicates the jump in ϕ_x across the discontinuity, and the subscript s denotes the quantity evaluated at the shock surface.

In two-dimensional small-perturbation transonic flows, the shock waves that usually occur are nearly normal to the flow direction. We assume here that if the basic steady flow has a shock wave then this shock may be approximated by a shock wave normal to the freestream flow. Furthermore, we assume that the motion of any shock wave that arises from unsteady changes in the flow, as well as the motion of existing shock waves, also may be calculated by this normal shock approximation. For this simplified model, Eqs. (3) and (4) reduce to the single equation

$$\left(\frac{dx}{dt}\right)_s=\frac{\gamma+1}{2K}\left\{\frac{M_\infty^2-1}{(\gamma+1)M_\infty^2}+\tilde{\phi}_x\right\} \quad (5)$$

which gives the speed of the normal shock in the flowfield. For steady flows, $\tilde{\phi}_x$ is a function of x alone; this, of course, still permits $[\![\phi_x]\!]$ to vary with y. For unsteady flows, although $\dot{x}_s$ is a function of t alone, the strength of the shock will still vary with y.

Coordinate Stretching

To minimize the far-field boundary effects on the numerical results, a relatively large computational region is usually required. For the cases studied in this paper, the shock excursion may be large and the unsteady disturbances carried several chord lengths away from the airfoil; thus, the use of a relatively large computational domain seems inevitable. A simple and straightforward way of computing the solution in a large computational domain is to use nonuniform mesh distributions, with most of the mesh points concentrated in the region of interest.[2] An alternative is to introduce analytical coordinate stretchings. In the present study, we use the following coordinate stretchings:

$$\xi=\pm\{1-\exp(\mp a_1x)\} \text{ for } x\gtrless 0 \quad (6a)$$

$$\eta=\pm\{1-\exp(\mp a_2y)\} \text{ for } y\gtrless 0 \quad (6b)$$

where a_1 and a_2 are constants that control the mesh distributions.¶ Equations (6) transform the infinite physical domain to the finite computational domain bounded by $|\xi|\le 1$ and $|\eta|\le 1$. The transformation provides a concentrated mesh distribution near the airfoil which is suitable for the present study. The governing Eq. (1), written in the stretched coordinate system, is

$$\left\{\frac{-2KM_\infty^2}{a_2^2(1-|\eta|)}\phi_\xi\right\}_t-\left\{\frac{(\gamma+1)M_\infty^2}{2a_2^2(1-|\eta|)}\left[\frac{M_\infty^2-1}{(\gamma+1)M_\infty^2}+a_1(1-|\xi|)\phi_\xi\right]^2\right\}_\xi+\left\{\frac{1-|\eta|}{a_1(1-|\xi|)}\phi_\eta\right\}_\eta=0 \quad (7)$$

Because Eq. (7) is in divergence-free form, a conservative difference approximation to Eq. (7) can be constructed if the shock wave is to be "captured" rather than "fitted."

The normal shock jump relation follows directly from Eq. (7); this relation and the boundary condition on the airfoil surface are now

$$\left(\frac{d\xi}{dt}\right)_s=\frac{a_1(1-|\xi|)(\gamma+1)}{2K}\left\{\frac{M_\infty^2-1}{(\gamma+1)M_\infty^2}+a_1(1-|\xi|)\tilde{\phi}_\xi\right\} \quad (8)$$

§In the cases studied numerically, $Y_{u_x}=O(Y_{u_t})$; consequently, the last term in Eq. (2) is of higher order and was neglected.

¶Calculations made with an algebraic scaling, viz., $\xi=x/(|x|+a_1)$, etc., gave essentially identical results.

and

$$\phi_\eta = \frac{a_1}{a_2}(1-|\xi|)\frac{\partial Y(\xi,t)}{\partial \xi} \text{ at } \eta = 0 \tag{9}$$

Scaling of the Perturbation Equation

In his study of steady, small-disturbance transonic flow, Krupp[21] introduced a scaling of the governing equation and the body shape to provide better agreement between the results of the perturbation calculations and those from the Euler equations. The reasoning that leads to various scalings is discussed in the review by Ballhaus.[22] One also may use such a scaling in the low-frequency approximation by rewriting the governing equation and the boundary condition as

$$-2KM_\infty^p \phi_{xt} + \{1 - M_\infty^2 - (\gamma+1)M_\infty^m \phi_x\}\phi_{xx} + \phi_{yy} = 0 \tag{10}$$

and

$$\phi_y = M_\infty^n \tau \left\{ Y_{s_x} + \frac{\delta}{M_\infty^n \tau} Y_{u_x} \right\} \tag{11}$$

where p, m, and n are scaling constants to be chosen to enhance agreement with more sophisticated calculations. If one introduces the nondimensional quantities

$$\bar{\phi} = \frac{(\gamma+1)^{1/3}}{M_\infty^{1/3(2n-m)}\tau^{2/3}}\phi \tag{12a}$$

$$\bar{y} = \{(\gamma+1)M_\infty^{m+n}\tau\}^{1/3} y \tag{12b}$$

$$\bar{t} = \{(\gamma+1)^2 M_\infty^{2m+2n-3p}\tau^2\}^{1/3} t/2K \tag{12c}$$

$$\alpha = \frac{1-M_\infty^2}{\{(\gamma+1)M_\infty^{n+m}\tau\}^{2/3}} \tag{12d}$$

$$\beta = \delta/M_\infty^n \tau \tag{12e}$$

then Eqs. (10) and (11) reduce to the canonical form

$$-\bar{\phi}_{x\bar{t}} + (\alpha - \bar{\phi}_x)\bar{\phi}_{xx} + \bar{\phi}_{\bar{y}\bar{y}} = 0 \tag{13}$$

and

$$\bar{\phi}_{\bar{y}} = Y_{s_x} + \beta Y_{u_x} \tag{14}$$

Because there is a one-to-one correspondence between Eqs. (1) and (2) and Eqs. (13) and (14), results obtained without scaling are equivalent to scaled calculations for a slightly different flow. Thus, although we restrict our calculations to the unscaled equation, the Mach number and the body shape can be modified to obtain results equivalent to those for the scaled equation by noting the equivalencies [Eqs. (12)].

Boundary Conditions

The boundary condition on the airfoil is the usual tangency condition evaluated at $y = 0$. For an NACA 64A006 airfoil with an oscillating quarter-chord flap, the boundary conditions are

$$\phi_y = \begin{cases} \tau Y_{s_x} & \text{for } 0 \le x \le 0.75 \\ \tau\left(Y_{s_x} + \dfrac{\delta}{\tau}\sin t\right) & \text{for } 0.75 < x \le 1 \end{cases}$$

With the proper combinations of the reduced frequency K, the free Mach number M_∞, and the oscillating amplitude δ, we can simulate the three types of shock motions observed experimentally by Tijdeman[13,14]: the shock oscillates on the airfoil (type A); the shock disappears during part of the period (type B); and the shock propagates upstream and leaves the airfoil (type C). The thickness distribution for an NACA 64A006 airfoil may be obtained from Ref. 23 and the desired airfoil slope at the grid locations approximated by fitting a polynomial to the data.

The far-field boundary condition for the nonlifting case is simply $\phi = 0$ on $|\xi| = 1$ and $|\eta| = 1$. For the lifting case, ϕ depends on the instantaneous circulation Γ. This dependence can be derived theoretically by assuming that in the far field all of the perturbations are small compared to the basic steady state.[24] An advantage of our stretched coordinate system is that the last grid lines are at infinity. Numerical studies conducted by Magnus[6] show that erroneous boundary data on a finite domain can lead to significant errors. The low-frequency approximation implies that any changes in the circulation are communicated instantly downstream to infinity ($\xi = 1$). Consequently, the simplest boundary conditions are $\phi_x = 0$ on the downstream boundary and $\phi = 0$ on the other boundaries. Ballhaus and Goorjian[2] used similar boundary conditions in their study and obtained satisfactory results. The validity of such far-field boundary conditions can be justified only by numerical experiments; i.e., near the boundary the disturbance quantities ϕ_x and ϕ_y must be much smaller than the values at the airfoil surfaces. In all of the results reported here, this requirement is met. As a numerical test of this procedure, we have computed the steady-state circulation about an NACA 64A006 airfoil for various flap deflection angles, using the ADI method with appropriate far-field values of ϕ corrected for the usual steady-state circulation contribution. These results have been compared with the results obtained by the ADI calculations with the boundary conditions employed here for an unsteady flap deflection to the correct angle. These results agree to one part in 10^{-4}, verifying that the far-field conditions used here are more than satisfactory.

Finite-Difference Approximations

In a preliminary study of the unsteady transonic flows, we implemented a normal shock-fitting procedure in the implicit-iterative scheme of Caradonna and Isom.[7] Satisfactory results were obtained, except that the procedure was time-consuming because of the iterative process required at each time step. The recent studies of Ballhaus and Steger[1] and Ballhaus and Goorjian[2] show that an ADI scheme is more efficient than the implicit-iterative scheme in treating the low-frequency transonic flow equation. The shock-fitting algorithm was modified and implemented with an ADI scheme. In this section, the ADI procedure is reviewed briefly and the method for unsteady shock fitting detailed.

Alternating-Direction Implicit (ADI) Method

The low-frequency equation in the stretched coordinate system, i.e., Eq. (7), is solved by the alternating-direction implicit scheme developed by Ballhaus and Steger.[1] To simplify this discussion, Eq. (7) is rewritten in the form

$$\psi_{\xi t} + F_\xi + G_\eta = 0 \tag{15}$$

where the functions ψ, F, and G may be determined by comparing Eqs. (7) and (15). The solution is advanced from time level n to level $n+1$ by the following two-step procedure:

ξ Sweep

$$(1/\Delta t)(\psi_\xi^+ - \psi_\xi^n) + D_\xi F^+ + \delta_\eta G^n = 0 \tag{16a}$$

η Sweep

$$(1/\Delta t)(\psi_\xi^{n+1} - \psi_\xi^+) + \tfrac{1}{2}\delta_\eta (G^{n+1} - G^n) = 0 \tag{16b}$$

Here a plus sign refers to an intermediate value of ψ, D_ξ is the type-dependent difference operator for ξ derivatives, and δ_η is the central-difference approximation for the η derivative. The

backward difference approximation for ψ_ξ can be either the first-order difference approximation

$$\psi_\xi = (1/\Delta\xi)(\psi_i - \psi_{i-1}) \tag{17}$$

or the second-order difference approximation

$$\psi_\xi = (1/2\Delta\xi)(3\psi_i - 4\psi_{i-1} + \psi_{i-2})$$

For simplicity the first-order scheme, Eq. (17), has been used for all of the results reported here. The nonlinear term F is evaluated, using a two-time-level averaging procedure analogous to that of Ballhaus and Steger[1] but modified by the coordinate stretching used here. The difference approximations described previously provide first-order accuracy for $\psi_{\xi t}$, second-order accuracy for F_ξ and G_η in subsonic regions, and first-order accuracy for F_ξ in supersonic regions.

On the ξ sweep, Eq. (16a), a quadradiagonal system is generated and can be solved easily by direct elimination. For lifting calculations, two grid lines are used to represent the lower and upper surfaces of the airfoil. The circulation Γ is calculated by $\Gamma = \phi^U_{ITE} - \phi^L_{ITE}$ through each sweep. Here ITE denotes the upper and lower values at the first grid point behind the trailing edge. This circulation is incorporated into the construction of the η derivatives behind the airfoil for $\eta = 0$.

On the η sweep, Eq. (16b), a tridiagonal system is generated on the body. Ahead of the leading edge and behind the trailing edge, the double grid notation for $\eta = 0$ destroys the tridiagonal system. However, ahead of the leading edge, $\phi^U = \phi^L$, and behind the trailing edge, $\phi^U = \phi^L + \Gamma$; thus the difference equations can be reordered to give a tridiagonal system. On the airfoil surface the matrix equations above and below the airfoil are decoupled; they can be solved either separately or simultaneously by packing the matrix equations together.

Shock-Fitting Procedure

The basic algorithm for shock fitting was developed in a previous study of steady transonic flows.[12] A different approach to shock fitting also has been developed by Hafez and Cheng[25] in their study of steady transonic flow problems. Their procedure essentially replaces the shock-point operator by an analogous difference statement derived from the shock jump conditions. Subsequently, the velocity potential on each side of the shock wave is extrapolated to locate the shock wave.

To understand the shock-fitting procedure for unsteady transonic flow calculations it is necessary to recall how shock waves form in an unsteady field. Shock waves are generated when the local flow becomes supersonic and compressive. Although the initial shock formation may not be predicted accurately by the numerical solution when shock fitting is used in the early stages of shock-wave formation, it eliminates spurious oscillations in the numerical solution and does provide the correct development of the shock wave in later stages of the calculations.[26] The criterion that we set for the initial shock formation is that the local flow become sonic (relative to the airfoil) and compressive. In the body-fixed coordinate system, a shock wave can exist both in the usual supersonic-supersonic and supersonic-subsonic transition and also in a purely subsonic flowfield, sometimes referred to as a "subsonic-subsonic" shock. In any case, the flow ahead of the shock relative to a coordinate system fixed on the shock must be always supersonic. Consequently, the correct judgment for the existence of a shock wave in the unsteady field is to evaluate the local flow velocity ahead of a prospective shock with respect to the coordinate system fixed on it, i.e., we evaluate V_r, where

$$V_r \approx \frac{M_\infty - 1}{M_\infty} + \left\{1 + \frac{(\gamma-1)M_\infty}{2}\right\} a_l (1 - |\xi|)\phi_\xi - \frac{K}{a_l(1-|\xi|)}\left(\frac{d\xi}{dt}\right)_s$$

If $V_r > 0$, the local flow is supersonic and a shock may exist; if $V_r \to 0^+$, the local flow becomes sonic and the shock strength diminishes. For $V_r \le 0$, a shock cannot exist.

We start the unsteady flow calculations by using an ADI scheme. When the local flow becomes sonic and compressive, we introduce the shock-fitting algorithm. Sonic, compressive points are treated as shock points where cross differentiations in t and ξ derivatives are avoided. Initially, the shock has zero strength and is stationary. The flow properties ahead of and behind the shock can be extrapolated easily from neighboring points. The shock wave can either increase or decrease in strength during the unsteady process. This results in three possibilities for shock motion that have to be considered separately in the fitting procedure: the shock moves upstream and crosses grid points; the shock remains stationary or moves within a grid spacing; and the shock moves downstream and crosses grid points. At each new time level the shock position is determined by applying Eq. (8). The formulations of the difference approximations for each case are quite similar; the specific formulas used may be found in Ref. 27.

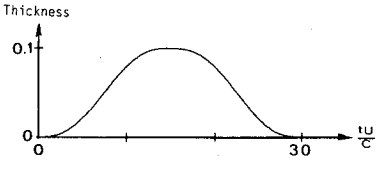

Fig. 1 Maximum thickness vs time for pulsating parabolic arc in units of percent thickness vs time in units of chord/speed.

Results and Discussion

To illustrate the advantages of shock fitting over shock capturing, we compare the flow past a pulsating parabolic arc whose time history is shown in Fig. 1, as computed by the two methods. Major differences occur when the shock wave propagates ahead of the airfoil as its thickness returns to zero. Figure 2 compares the pressure coefficient for these later stages when $t \ge 25$ (chord/U) in units of $\Delta t = 2$ computed by the ADI method, with and without shock fitting. The full time history of this motion, as computed by the two methods, is compared in Ref. 27. Later studies have shown, as suggested by a reviewer, that the compression preceding the fitted shock wave is a result of the first-order approximation made here. In subsequent calculations with a second-order procedure, which is possible with shock fitting, this behavior does not occur.

Results were computed for an NACA 64A006 airfoil with quarter-chord oscillating flap for various values of the reduced frequency K, the freestream Mach number M_∞, and the oscillation amplitude δ, in order to simulate the shock motions observed by Tijdeman.[13,14] The steady-state solutions at the mean flap deflection angle for each M_∞ are computed first, using the ADI method of shock fitting. We have found that the ADI scheme is more efficient than successive over-relaxation in computing steady flows. The results of the ADI calculations are identical with those obtained by line relaxation and converge more rapidly when performed with the stretched coordinates. For the problems studied here, i.e., the NACA 64A006 airfoil, the freestream Mach number was varied between 0.8 and 0.9. The mesh system had 101 by 82 grid points in the x and y directions, respectively. About 250 to 450 time steps were required for the solution to converge, $|\Delta\phi|_{max} \le 10^4$. Thse steady-state solutions are used as initial data for the unsteady flow calculations. For all cases

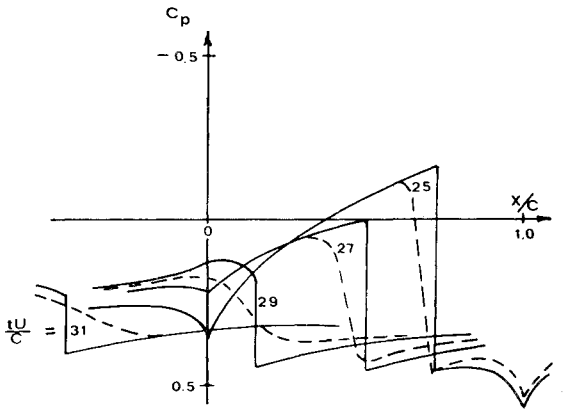

Fig. 2 Pressure coefficient in the later stages of the motion of Fig. 1 computed with (——) and without (---) shock-fitting.

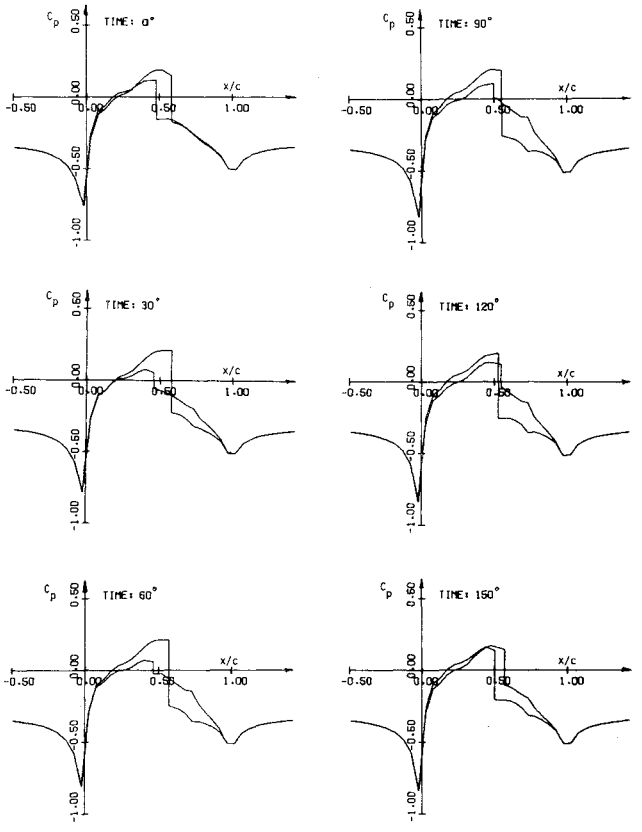

Fig. 3 C_p on an NACA 64A006 airfoil at $M_\infty = 0.854$, $K = 0.358$, with δ = 1-deg sin$t$.

studied it took three to six cycles for the flowfield to become periodic. Stability seems to require that the time step Δt be small enough that Δt (deg)$/K < 10$. Figure 3 illustrates the pressure coefficients on the airfoil surface for $M_\infty = 0.854$, $K = 0.358$, and δY_{u_X} = 1-deg sin$t$. For these conditions, Ballhaus and Goorjian[2] were able to simulate type B motion where the shock disappears during some part of the cycle. Here the shock does not disappear during the cycle; instead, it becomes quite weak during a small portion of the cycle. This difference is due to the assumption of a normal shock, which results in a stronger shock than would normally occur, and to the use of shock fitting. Magnus and Yoshihara's explicit results for the full Euler equations are compared with these results for two time levels in Fig. 4. The discrepancy between the two results is due mainly to the small-disturbance approximation and the lack of resolution at the leading edge of the present study. Figure 5 shows the time history, during the

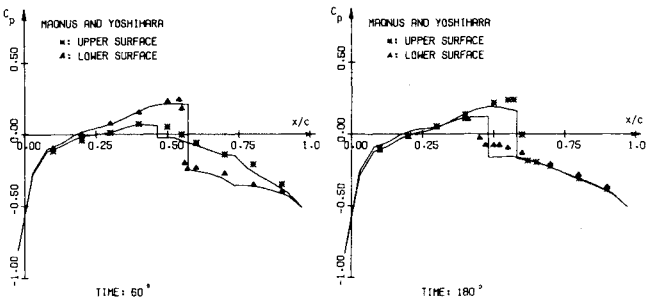

Fig. 4 Comparisons of the results for C_p on an NACA 64A006 airfoil at $M_\infty = 0.854$, $K = 0.358$, with δ = 1-deg sin$t$, with those of Magnus and Yoshihara.[4,5]

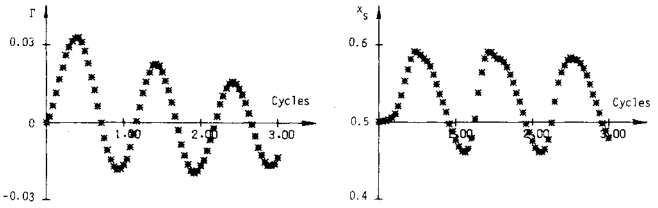

Fig. 5 History of the circulation and shock position for the first three cycles for the flow conditions of Fig. 3.

first three cycles, of the circulation and the shock position. After three cycles of oscillation, the pressure field is essentially periodic; the circulation requires four cycles to become periodic. The circulation reaches its maximum value, and the shock wave its most downstream location, 57 and 83 deg after full flap deflection. Results for type C motion are given in Ref. 27 and hence not repeated here.

The results for $M_\infty = 0.822$, $K = 0.496$, and $\delta Y_{u_X} = 2$ deg sin$t$ simulate type C shock motion. Because we have used less spatial resolution and the unscaled equation, a deflection angle slightly larger than that of Ref. 2 is needed in order to generate the type C shock motion; that is, we need a 2-deg deflection angle rather than the 1.5 deg used in Ref. 2 to get analogous behavior. The results are given in Ref. 27. In this case, the flowfield is subcritical during most of the cycle, and the shock wave is barely "captured" in the non-shock-fitting procedure. During the unsteady process, the shock wave moves toward the leading edge. The strong singular behavior in pressure at the leading edge prevents the shock from propagating off the airfoil. The perturbation velocity becomes large and is negative; thus, the flow used to calculate the relative velocity ahead of the shock can no longer support a shock wave. Normal shock-fitting calculations determine the shock speed from the pressure jump across the shock at the airfoil surface. This eliminates the possibility that a portion of the shock may propagate off the leading edge in the computations. But this does not imply that it cannot occur; instead this limitation is a consequence of the normal shock fitting.

The addition of the shock-fitting algorithm to the basic ADI scheme increased the computational time, for fixed grid spacing, by less than 7% for all cases studied here. It is difficult to compare the time required by the two schemes to achieve the same accuracy. Without shock fitting, when the shock is not of the supersonic-subsonic type, a very fine grid is required for a reasonable resolution at the shock. The need for such a grid is obviated by shock fitting, and improved accuracy in the shock region can be obtained simultaneously with reduced computational time. Because it is difficult to determine when the two procedures give comparable accuracy, a definitive evaluation of the computing time saved by shock fitting has not been attempted.

Typical computation times for the NACA 64A006 airfoil calculations reported here are about 5 to 10 min/cycle on a

CDC 6400 computer. A mesh of 101 by 82 grid lines in x and y directions, respectively, was used in these calculations, and the number of time steps per cycle ranged from 90 to 180. No effort was made to optimize the program. The additional central memory required for the shock-fitting algorithm is about 10 to 20% of that for the basic ADI scheme.

Conclusion

The unsteady behavior of a large number of inviscid low-frequency transonic flows can be studied accurately and efficiently using the present shock-fitting procedure coupled with the alternating-direction implicit method. The ADI method relaxes the stability restriction on the time step, greatly improving the computational efficiency; the shock-fitting procedure treats shock waves as discontinuities, which resolves the computational difficulties that can arise in the usual shock "capturing" procedure. Computed results using the present procedure compare favorably with the explicit time integrations carried out by Magnus and Yoshihara. They should be sufficiently accurate for engineering studies of airfoil motions for which the normal shock approximation made here is a reasonable one. They also reproduce well the types of shock motions observed experimentally by Tijdeman,[13,14] as well as the propagation of the shock wave ahead of the pulsating parabolic arc.

Acknowledgment

This research was sponsored by NASA through Grant NSG-2112 and the Air Force Office of Scientific Research through Grant 76-2954.

References

[1] Ballhaus, W. F. and Steger, J. L., "Implicit Approximate-Factorization Schemes for the Low-Frequency Transonic Equation," NASA TM X-73082, 1975.

[2] Ballhaus, W. F. and Goorjian, P. M., "Implicit Finite Difference Computations of Unsteady Transonic Flows about Airfoils," *AIAA Journal*, Vol. 15, Dec. 1977, pp. 1728-1735.

[3] Ballhaus, W. F. and Lomax, H., "The Numerical Simulation of Low Frequency Unsteady Transonic Flow Fields," *Lecture Notes in Physics*, Vol. 35, Springer-Verlag, Berlin, 1975, pp. 57-63.

[4] Magnus, R. and Yoshihara, H., "Unsteady Transonic Flows Over an Airfoil," *AIAA Journal*, Vol. 13, Dec. 1975, pp. 1622-1628.

[5] Magnus, R. and Yoshihara, H., "The Transonic Oscillating Flap," AIAA Paper 76-327, 1976.

[6] Magnus, R. J., "Computational Research on Inviscid, Unsteady, Transonic Flow over Airfoils," Office of Naval Research, Rept. CASD/LVP 77-010, 1977.

[7] Caradonna, F. X. and Isom, M. P., "Numerical Calculation of Unsteady Transonic Potential Flow Over Helicopter Rotor Blades," *AIAA Journal*, Vol. 14, April 1976, pp. 482-488.

[8] Beam, R. M. and Warming, R. F., "An Implicit Finite-Difference Algorithm for Hyperbolic Systems in Conservation-Law Form," *Journal of Computational Physics*, Vol. 22, Jan. 1976, pp. 87-110.

[9] Traci, R. M., Albano, E., and Farr, J. L., "Perturbation Method for Transonic Flows about Oscillating Airfoils," *AIAA Journal*, Vol. 14, Sept. 1976, pp. 1258-1265.

[10] Weatherill, W. H., Ehlers, F. E., and Sebastian, J. D., "Computation of the Transonic Perturbation Flow Fields Around Two- and Three-Dimensional Oscillating Wings," NASA CR-2599, 1975.

[11] Ballhaus, W. F. and Goorjian, P. M., "Computation of Unsteady Transonic Flows by the Indicial Method," *AIAA Journal*, Vol. 16, Feb. 1978, pp. 117-124.

[12] Yu, N. J. and Seebass, A. R., "Inviscid Transonic Flow Computations with Shock Fitting," *IUTAM Symposium Transsonicum II*, edited by K. Oswatitsch and D. Rues, Göttingen, Germany, 1975, pp. 449-456.

[13] Tijdeman, H., "On the Motion of Shock Waves on an Airfoil with Oscillation Flap in Two-Dimensional Transonic Flow," NLR TR 75038U, 1975.

[14] Tijdeman, H., "On the Motion of Shock Waves on an Airfoil with Oscillating Flap," *IUTAM Symposium Transsonicum II*, edited by K. Oswatitsch and D. Rues, Göttingen, Germany, 1975, pp. 49-56.

[15] Hafez, M. M., Rizk, M. H., and Murman, E. M., "Numerical Solution of the Unsteady Transonic Small-Disturbance Equations," *AGARD Meeting*, Lisbon, Portugal, April 1977.

[16] Fung, K-Y., Yu, N. J., and Seebass, A. R., "Small Unsteady Perturbations in Transonic Flows," to be published in *AIAA Journal*.

[17] Ballhaus, W. F., Jameson, A., and Albert, J., "Implicit Approximate-Factorization Schemes for Steady Transonic Flow Problems," AIAA Paper 77-634, 1977; also *AIAA Journal* (to be published).

[18] Yu, N. J. and Seebass, A. R., unpublished results, 1976.

[19] Jameson, A., "Iterative Solution of Transonic Flows Over Airfoils and Wings, Including Flows at Mach 1," *Communications in Pure and Applied Mathematics*, Vol. 27, 1974, pp. 283-309.

[20] Lin, C. C., Reissner, E., and Tsien, H. S., "On Two-Dimensional Non-Steady Motion of a Slender Body in a Compressible Fluid," *Journal of Mathematics and Physics*, Vol. 27, March 1948, pp. 220-231.

[21] Krupp, J. A., "The Numerical Calculations of Plane Steady Transonic Flows past Thin Lifting Airfoils," Boeing Scientific Research Lab., Rept. 0180-12958-1, 1971.

[22] Ballhaus, W. F., "Some Recent Progress in Transonic Flow Computations," *VKI Lecture Series on Computational Fluid Dynamics*, 1976.

[23] Abbott, I. H. and von Doenhoff, A. E., *Theory of Wing Sections*, McGraw-Hill, New York, 1949, Appendix I, p. 354.

[24] Krupp, J. A. and Cole, J. D., "Studies in Transonic Flow IV, Unsteady Transonic Flow," Univ. of California at Los Angeles, Engineering Rept. 76104, 1976.

[25] Hafez, M. M. and Cheng, H. K., "Convergence Acceleration and Shock Fitting for Transonic Aerodynamics Computations," AIAA Paper 75-51, 1975.

[26] Moretti, G., "Thoughts and Afterthoughts about Shock Computations," Polytechnic Inst. of Brooklyn, PIBAL Rept. 72-37, 1972.

[27] Yu, N. J., Seebass, A. R., and Ballhaus, W. F., "An Implicit Shock-Fitting Scheme for Unsteady Transonic Flow Computations," AIAA Paper 77-633, 1977, pp. 13-26.